Biosensors and Bioelectronics 138 (2019) 111316

Contents lists available at ScienceDirect

Biosensors and Bioelectronics

journal homepage: www.elsevier.com/locate/bios

Specific cell capture and noninvasive release via moderate electrochemical oxidation of boronic ester linkage

Qian-Wen Zhang, Jun Ouyang, Yang Wang, Ting-Ting Zhai, Chen Wang, Zeng-Qiang Wu, Tian-Qi Zhang, Kang Wang, Xing-Hua Xia*

State Key Laboratory of Analytical Chemistry for Life Science, School of Chemistry and Chemical Engineering, Nanjing University, Nanjing, 210023, China

ARTICLE INFO

Keywords:
CTCs
Cell capture
Electrochemical release
Boronic ester linkage

ABSTRACT

Early diagnosis and therapy of cancer metastasis are of great importance for disease outcome. Circulating tumor cells (CTCs) offer the ability for noninvasive tumor profiling in real time. However, simply capturing and counting tumor cells are inadequate to provide valuable information about tumor. Efficiently releasing the captured cells is necessary for the downstream characterization. Herein, we describe a mild electrochemical strategy to effectively isolate CTCs from the bloodstream and rapidly release the captured cells in 2 min for downstream molecular characterization, as realized on a conductive poly(aminophenylboronic acid) derivatized electrode. The boronic ester linkage between dopamine (DA) and boronic acids-functionalized electrode is stable, and only upon the application of a weak potential perturbation does the boronic ester dissociate and release cells without compromising cell viability. This platform is reusable after acid treatment and has the potential to be the next-generation platform for cell capture and release, realizing the clinical value of CTCs as biomarkers.

1. Introduction

Circulating tumor cells (CTCs) escape from the primary tumor site and enter into blood circulation, carrying important information of cancer development and metastasis (Plaks et al., 2013). Compared with biopsy, the widely used approach for cancer diagnosis, CTCs offer noninvasive and convenient access to tumor cells before fatal metastasis happens (Chambers et al., 2002). Therefore, isolation and detection of CTCs from the bloodstream hold great importance for examining metastasis, monitoring drug response, and assessing therapeutic results (Yoon et al., 2014). Given the functional diversity of CTC subtypes, most of the existing technologies are to capture and enumerate CTCs, which provide limited insights into the mechanism of tumor biology and cancer metastasis (Green et al., 2016). The recent research has been focusing on the phenotypic characterization of heterogeneous CTC subtypes (Labib et al., 2016; Poudineh et al., 2017; Schiro et al., 2012), demanding for an appropriate platform that can capture CTCs and efficiently release the attached cells. Many efforts have been made to release the immobilized cells from capture substrate triggered by enzymatic reaction (Shah et al., 2012), light (Lee et al., 2015; Liu et al., 2009), temperature (Ao et al., 2015; Hou et al., 2013; Reategui et al., 2015), or solution pH (Li et al., 2013; Liu et al., 2013). Despite great progresses being made, these approaches yet have their limitations. For pH-responsive surfaces, they require precise manipulation of the system pH to obtain uniform recovery of the cells and take relatively longer time to release the adhered cells. The use of enzymes would cleave cell-surface proteins, which might destroy the functions of CTCs (Li et al., 2015). Therefore, isolating CTCs from large populations of cells and acquiring detailed analyses for early detection and therapy of cancer are remaining challenges (Parkinson et al., 2012; Robertus et al., 2010).

Different from the above approaches, electrochemical methods have been conceived as an alternative way for cancer cell analysis (Persson et al., 2011; Wischerhoff et al., 2008; Zhang et al., 2013). They permit easy manipulation of cell adhesion by tuning electrochemical parameters of potential or current with high sensitivity, while requiring simple instruments and negligible hand-on time, which would further facilitate commercialization of these devices (Gao et al., 2016; Ng et al., 2012; Wan et al., 2014). However, current electrochemical approaches require a very negative potential of −1.2 V to release attached cells. This potential applied to cleave Au–S bond to release captured CTCs might bring damages to cells.

In recent years, boronic acids-containing polymers have been widely used in sensing (James et al., 1996; Nishiyabu et al., 2011), separation (Nie et al., 2013), drug delivery (Chen et al., 2012; Li et al.,

* Corresponding author.
E-mail address: xhxia@nju.edu.cn (X.-H. Xia).

https://doi.org/10.1016/j.bios.2019.111316
Received 24 February 2019; Received in revised form 7 May 2019; Accepted 9 May 2019
Available online 10 May 2019
0956-5663/

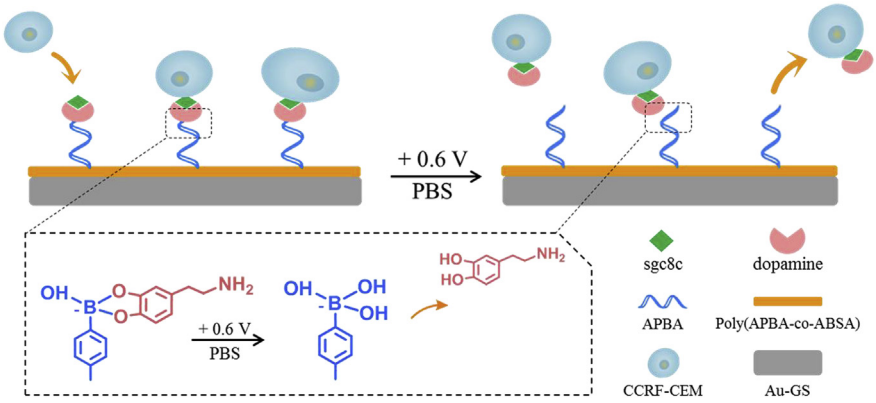

Scheme 1. Illustration of the modification of sgc8c aptamer on an electroactive, phenylboronic acid functionalized poly(APBA-co-ABSA) platform for the specific capture of CTCs and subsequent release of the adhered cells through an electrochemical cleavage of borate ester between dopamine and phenylboronic acid on the substrate.

2012) and controllable cell capture and release owing to the reversible covalent binding between boronic acids and diols (Zhong et al., 2010). We have previously established a synthetic strategy to generate poly (aminophenylboronic acid) (polyAPBA) with different fractal dimensions, which dramatically improves the capture efficiency of CTCs via the synergistic effect of chemical and topographical interactions (Ouyang et al., 2015). However, under neutral conditions, the polyAPBA exhibits insufficient conductivity for practical application of electrochemical biosensing. This limitation can be overcome by the incorporation of sulfonic acid groups into polyAPBA (Jiang and Epstein, 1990).

Herein, we for the first time demonstrate a noninvasive potential-mediated interface which can rapidly switch between capture and release of target CTCs through an electrochemical cleavage of borate ester bond at moderate voltage bias. The polyAPBA doped with aminobenzenesulfonic acid (poly(APBA-co-ABSA)) is applied as the conductive polymer scaffold for cell capture and release. The modification of poly(APBA-co-ABSA) and the procedure for attachment and detachment of CTCs on the surface of poly(APBA-co-ABSA) modified electrode are presented as Scheme 1. Briefly, dopamine (DA) is conjugated to the poly(APBA-co-ABSA) substrates through the boronate affinity to the boronic acid (Wang et al., 2014). The as-synthesized polymer scaffold is terminated with amine groups that can be readily interacted with aptamer leading to a high efficiency for cell capture. The DA bound to the surfaces can be specifically and rapidly broken by applying a moderate potential onto the polymer scaffold, resulting in the fast release of the DA and attached cells. Compared with the pH-dependent dissociation of borate ester in previous studies (Ivanov et al., 2006), our electrochemical strategy can efficiently release the adhered cells in 2 min with 98% cell viability through the mild electrical stimulation. The fast and noninvasive cell release achieved in our approach makes it possible to realize high-throughput detection of CTCs in the clinical application. Besides, the noninvasive potential-mediated interface can be repeatedly utilized. Therefore, this strategy is promising to facilitate the clinical application of CTCs as a liquid biopsy and disclose the molecular signature of a tumor.

2. Material and methods

2.1. Reagents and materials

Sulfuric acid, hydrochloric acid, hydrogen peroxide, sodium fluoride and ammonium persulfate were obtained from Nanjing Chemical Reagent Co. Ltd. (China). 2-Aminobenzenesulfonic Acid (ABSA) and 3-Aminophenylboronic acid (APBA) were purchased from TCI Development Co. Ltd. (China). Gold film coated glass slide (Au-GS) used as the working electrode for polymerization of APBA were purchased from Haoyue Quartz Co. (China). Penicillin-streptomycin and fetal bovine serum (FBS) were purchased from Corning Inc. Propidium iodide (PI), acridine orange (AO), RPMI-1640 culture medium and phosphate buffered saline (PBS, pH 7.4) were purchased from KeyGEN BioTECH development Co. Ltd. CellTracker Deep Red were purchased from Thermo Fisher Scientific Co. Ltd. The CCRF-CEM and K562 cell lines were purchased from Shanghai Institutes for Biological Sciences (China). 5′-ATC TAA CTG CTG CGC CGC CGG GAA AAT ACT GTA CGG TTA GAT TTT TTT TTT-3'-$(CH_2)_3$-NH_2 aptamer (sgc8c) was purchased from Sangon Biotech Co. Ltd. (China). All aqueous solutions were prepared using ultrapure water (Millipore Milli-Q system).

2.2. Synthesis and modification of poly(APBA-co-ABSA) nanostructures

Poly (APBA-co-ABSA) was synthesized by traditional three-electrode system using an Au-GS as the working electrode. A platinum wire and a KCl saturated Ag/AgCl were used as the counter electrode and the reference. After sonication in ultrapure water and ethanol for 5 min respectively, the Au-GS was soaked in H_2O_2/H_2SO_4 solution (volume ratio 1:3) at 100 °C for 1 h and then cleaned with ultrapure water and dried. Electrochemical polymerization was carried out in a solution of 0.05 M APBA monomer, 0.05 M ABSA monomer and 0.2 M NaF prepared in 1 M H_2SO_4. The poly(APBA-co-ABSA) was polymerized by cyclic voltammetry with a potential window ranging from −0.1–1.1 V and characterized by cyclic voltammetry with a potential window ranging from 0 to 0.8 V. When a stable current-potential profile was reached, the poly (APBA-co-ABSA) nanostructures were electrochemical oxidized at a potential of 0.6 V for 120 s. After rinsing with the EDC/NHS for 1 h and 100 mM 4-dicarboxybenzene, the nanostructures were immersed in 100 mM dopamine in 0.1 M PBS (pH 7.4) to generate boron ester bond. Following a rinse with 2.5% glutaric dialdehyde for 2 h and 0.1 M PBS, the dopamine-modified nanostructures were immersed in 10 mM sgc8c at 4 °C overnight and then passivated in 1% BSA. The impedance measurements were carried out by a PGSTAT 302 system (Autolab).

2.3. Electrochemical oxidization of boron ester bond

To characterize the formation of boron ester bond, differential pulse voltammetry was measured by using working electrode in the 0.1 mM PBS containing 1 mM dopamine (pH 7.4) within a potential range from −0.3–0.8 V. As a control, another working electrode was immersed in 100 mM dopamine for 20 min and washed with PBS prior to measurement. Afterwards, DPV was taken for electrochemical oxidization of the boron ester bond within a potential window ranging from 0.4 to 0.8 V.

2.4. Attenuated total reflection-infrared spectroscopy

A gold film was coated onto the ZeSn prism by chemical deposition. Aptamer-modified poly (APBA-co-ABSA) was then assembled onto the Au-ZeSn prism. The prism incubated with 100 mM dopamine for 20 min

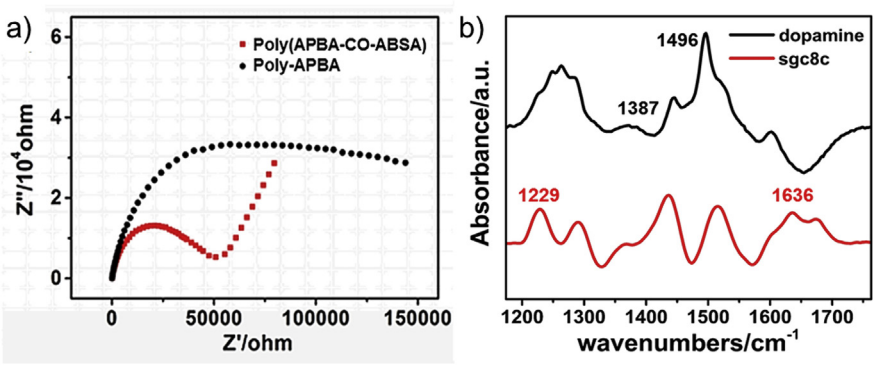

Fig. 1. a) Electrochemical impedance spectra of the poly (APBA-co-ABSA) (grey) and poly-APBA (black) modified electrode in 0.1 M PBS (pH 7.4) using $K_3Fe(CN)_6/K_4Fe(CN)_6$ as the electrochemical probe. b) ATR-IR spectra of dopamine (black) and sgc8c aptamer (grey) modifications using poly(APBA-co-ABSA) and DA-poly(APBA-co-ABSA) interfaces as the reference, respectively.

and washed with PBS was taken as the reference. After the application of a potential of 0.60 V for 120 s to the prism, the spectroscopy was recorded. The ATR-IR spectroscopy was performed by a Nicolet iS50 Fourier transform spectrometer (Thermo Fisher) with a liquid-nitrogen-cooled MCT detector. The spectral range was 4000–1000 cm^{-1} at 4 cm^{-1} resolution.

2.5. Cell culture

K562 and CCRF-CEM cells were cultured in RPMI-1640 medium containing 10% serum, streptomycin (0.08 mg mL^{-1}), glucose (2 g L^{-1}), penicillin (80 U mL^{-1}), L-Glutamine (0.3 g L^{-1}), and sodium bicarbonate (2 g L^{-1}) at 37 °C under 5% CO_2.

2.6. Cell capture and release assay

For cell capture, CCRF-CEM cells was centrifuged and redispersed in PBS solution (pH 7.4) to generate cell density of 1.8×10^4 cells/mL. A 20 μL as-prepared cell solution was incubated on the poly(APBA-co-ABSA) substrate (0.5 cm × 0.5 cm) at 37 °C for 60 min. For the blood sample analysis, blood cells were stained with CellTracker Deep Red and CCRF-CEM cells were stained with AO. CCRF-CEM cells were added into the blood sample (1×10^9 cells/mL) at a concentration of 5000 cells/mL. A 20 μL as-prepared cell solution was incubated on the poly(APBA-co-ABSA) substrate (0.5 cm × 0.5 cm) at 37 °C for 60 min. The substrate was gently washed with PBS to get rid of unconjugated cells for three times. Then, the captured cells were stained by Fluorescein dye AO and imaged and counted using a fluorescence inversion microscope (Nikon, TI-U). The release of the captured cells was achieved by applying a potential of 0.60 V for 120 s, 100 s and 80 s to the substrate, respectively. The substrate was rinsed in PBS solution (pH 7.4) during the electrochemical release of cells. We observed and counted the cells before and after release using an inversion microscope combined with electrochemical impedance spectroscopy. To verify the specificity of the substrate, the CCRF-CEM and K562 cell suspensions (20 μL, 2.5×10^6 cells/mL) were incubated on the substrates for 1 h followed by washing with PBS for three times and observed by fluorescence imaging.

2.7. Cell viability assay

Cell viability was measured by staining the captured cells with both Fluorescein dye AO and PI before and after release. After being captured on the substrate, the cells were rinsed into an AO/PI solution for 5 min and imaged by using an inversion microscope. The detached cells were collected, stained by AO/PI and also imaged by fluorescence imaging.

2.8. Characterization of the tyrosine kinase 7

6-AFM labelled sgc8c aptamer (Sangon Biotech) was used to monitor the tyrosine kinase 7 on the surface of CCRF-CEM cells. After release from the poly(APBA-co-ABSA) substrate, CCRF-CEM cells were incubated with 10 μM 6-AFM modified sgc8c aptamer for 30 min. After centrifuged at 1000 rpm for 5 min and resuspended in PBS, the cells were observed by fluorescence imaging.

3. Results

3.1. Synthesis and modification of poly(APBA-co-ABSA) nanostructures

The poly(APBA-co-ABSA) surface contains polymer chains, which are flexible to enhance the topographical interaction with CTCs (Liu et al., 2013). The doping with protonic acid improves the conductivity of this polymer in neutral condition (detailed synthetic procedures are provided in the supporting information, [SI]) (Kuralay et al., 2012). The poly(APBA-co-ABSA) has been characterized by ATR-IR. As shown in Fig. S2,a prominent peak at 1277 cm^{-1} attributing to the benzene ring vibration of APBA and ABSA can be observed. The band at 1480 cm^{-1} is assigned to the B–O stretching vibration of APBA. Besides, the positive peak at 1644 cm^{-1} is derived from the –OH bending vibration of APBA. The presence of ABSA is indicated by the peak at 1200 cm^{-1}, which is assigned to the $–SO_3$ stretching vibration. These results indicate that we have successfully synthesized the poly(APBA-co-ABSA) by chemical deposition. We then used electrochemical impedance spectroscopy (EIS) to characterize the self-doping with the change of charge transfer resistance (R_{ct}). After being doped with ABSA, the modified polymer shows a sharply decreased R_{ct} (Fig. 1a), indicating that the sulfonic acid self-doping can efficiently improve the substrate conductivity. The ratio of APBA to ABSA and the electrodepositing potential are the two major factors influencing the conductivity of the polymer. An increase in the relative content of ABSA improves the conductivity (Fig. S3a), which however makes it water-soluble and difficult to be deposited on the electrode. As a result, the ratio 1:1 is found to be optimal for the electrosynthesis of self-doped APBA. In our experiment, a minimum polymerization potential of 1.0 V (all potentials are referred to Ag/AgCl electrode with saturated KCl if not specified) is required in order to provide enough phenylboronic groups to capture CTCs. Higher deposition potential will thicken the polymer, thereby decreasing the conductivity of the substrate (Fig. S3b) and the deposited polymer would suffer degradation (Karyakin et al., 1994). Considering all these factors, a potential of 1.0 V is found to be sufficient to polymerize the optimal self-doped poly(APBA-co-ABSA) surface.

The poly(APBA-co-ABSA) surface is sequentially modified with DA, glutaraldehyde (GA) and sgc8c. DA can be easily immobilized on the boronic acids-containing poly(APBA-co-ABSA) surface because of boronate affinity. GA is then covalently attached to DA, functioning as a linkage to graft sgc8c. Finally, the surface is blocked with bovine serum albumin (BSA) to prevent non-specific adsorption. The stepwise modification of the poly(APBA-co-ABSA) surface has been confirmed by attenuated total reflection-infrared spectroscopy (ATR-IR) as shown in

Fig. 1b. The modification of DA results in the appearance of strong absorption at 1496 cm^{-1} assigning to the benzene ring vibration of DA. In addition, the positive band at 1387 cm^{-1} is attributed to the B–O stretching of boronic ester bond between phenylboronic group on poly (APBA-co-ABSA) surface and hydroxyl group of DA, indicating that DA has been covalently bound to the substrate. Sequential immobilization of sgc8c to the substrate is evidenced by the appearance of two positive bands at 1229 and 1636 cm^{-1} using the DA modified interface as the reference, which are derived from the PO_2^{-1} stretching mode and the C═N stretching mode induced by the formation of aldimine linkages between the amide groups of sgc8c and the aldehyde groups of GA, respectively.

3.2. Cell capture

Following the fabrication of the substrate, we evaluate the cell adhesion ability of the surface using human leukemic lymphoblasts (CCRF-CEM) as the targeted cell line. The sgc8c-modified poly(APBA-co-ABSA) surfaces were incubated in cell suspensions (20 μL, 1.8×10^4 cells mL^{-1}) for 60 min, at which the maximum capture yield is achieved. Characteristics of cell adhesion were analyzed by fluorescence microscopy (Fig. 2a). The capture yield reaches 83% in 60 min, indicating that the poly(APBA-co-ABSA) surface show good cell capture performance. Furthermore, to testify the specificity of the sgc8c-modified poly(APBA-co-ABSA) surface, we used K562 cell line as a control. Sgc8c can selectively bind to protein tyrosine kinase 7, which is highly expressed on the surface of CCRF-CEM cells but barely on the surface of K562 cells. It can be seen that numerous amounts of CCRF-CEM cells attach themselves to the sgc8c-modified poly(APBA-co-ABSA) surfaces (Fig. S4a), whereas K562 cells show very low non-specific cell attachment on the surfaces (Fig. S4b). These results verify that our designed surfaces have high specificity to capture CCRF-CEM cells. Additionally, 100 CCRF-CEM cells were added into the blood sample to verify the capability of the substrate for practical application. As shown in Fig. 2b, the existence of blood cells on the substrate indicates that the interference from other molecules in the blood cannot be avoided. Although CCRF-CEM cells can still be efficiently captured, the capture yield of the substrate decreases to 53% due to the nonspecific adsorption of blood cells.

3.3. Electrochemical oxidization of boron ester bond

We then attempt to electrochemically release the cells from the sgc8c-modified poly(APBA-co-ABSA) surfaces. Before that, we explored whether the moderate potentials can dissociate boronic ester bond, which will further lead to the release of DA. Specific binding between DA and the substrate was characterized by differential pulse voltammetry (DPV). All of the DPVs (Fig. 3a) were conducted in 0.1M PBS solution (pH 7.4) at a scan rate of 20 mV S^{-1}. The strong anodic peak of the poly(APBA-co-ABSA)-modified electrode at 0.0 V is due to the electric assisted deprotonation process of boronic acid (Wang et al., 2013). When DA is added in the solution, apart from the oxidation peak of DA in the solution phase located at 0.27 V, a new oxidation peak appears at 0.56 V which is not detected in the DPV of pristine poly (APBA-co-ABSA)-modified electrode (Fig. 3a, **black curve**). This oxidation peak is attributed to the oxidation of the boronate ester formed between DA and the boronic acid functionalized poly(APBA-co-ABSA), as the oxidation potential of boronate ester is much more positive than those necessary to oxidize free DA under physiological conditions (Huang et al., 2010). In addition, the electric assisted deprotonation peak decreases significantly owing to the dynamic blockage of the boronic acid by DA in solution. To verify the detachment of DA, the poly(APBA-co-ABSA)-modified electrode was immersed into 100 mM DA for 20 min and followed by washing with PBS before measurement. The oxidation peak for boronate ester at 0.56 V (Fig. 3a, **blue curve**) occurs only in the first scan. This peak disappears in the second scan, indicating successful dissociation of the boronate ester (Fig. S5) (Zhang et al., 2009). The appearance of a large deprotonation peak implies that not all the boronic acid is chemically bounded by DA. Importantly, the poly(APBA-co-ABSA) surface keeps stable over continuous potential scans and reusable since the original binding sites for DA can be easily restored by acid treatment after use (Wu et al., 2007).

To gather supporting evidence, we used ATR-IR to explore the intramolecular interactions within poly(APBA-co-ABSA)/DA at different potentials. The gold-coated IR prism was modified with poly(APBA-co-ABSA) using the aforementioned method. The DA-modified poly(APBA-co-ABSA) rinsed in 10 mM PBS was taken as the reference. In this manner, the spectra comprise the contributions from the changes of poly(APBA-co-ABSA) and DA induced by external electric field. Upon applying a potential of 0.6 V for 120 s, prominent negative bands at 1496 and 1387 cm^{-1} assigned to the benzene ring vibration of DA and the B–O stretching of boronic ester bonds are observed, indicating the detachment of DA molecules from the substrate (Fig. 3b**, black curve**). Their peak intensities are almost the same as those from the spectrum of DA modification (**red curve**), indicating that nearly all of the chemically bounded DA molecules are released in 2 min in response to the electrical stimulation.

3.4. Cell release and viability analysis

For subsequent cell release, the potential applied should be relatively mild to prevent the mammalian cells from being damaged by extreme electrical stimulation.[22] Therefore, the release of cells was performed at 0.6 V and characterized by fluorescence microscopy. The sgc8c-modified poly(APBA-co-ABSA) surfaces were rinsed in cell suspension for 60 min and non-specifically bound cells were removed by repeated washing. When the potential of 0.6 V is applied for 120 s, 88% cells are detached from the surfaces rapidly (Fig. 4). The time for applying the potential has been optimized. After applying a potential of 0.6 V for 100 s and 80 s to the substrate, only 75% and 40% cells are

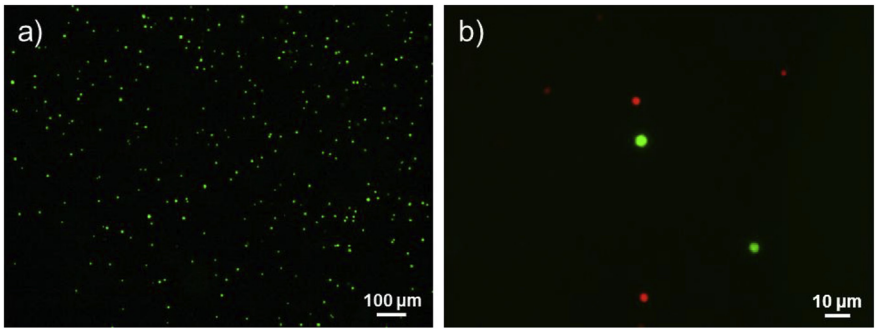

Fig. 2. a) Fluorescence images of CCRF-CEM cells captured on the sgc8c-modified poly(APBA-co-ABSA) surfaces. The maximum cell capture yield (83%) is achieved at 60 min. b) Fluorescence images of CCRF-CEM cells (stained green) in blood cell (stained blue) sample.

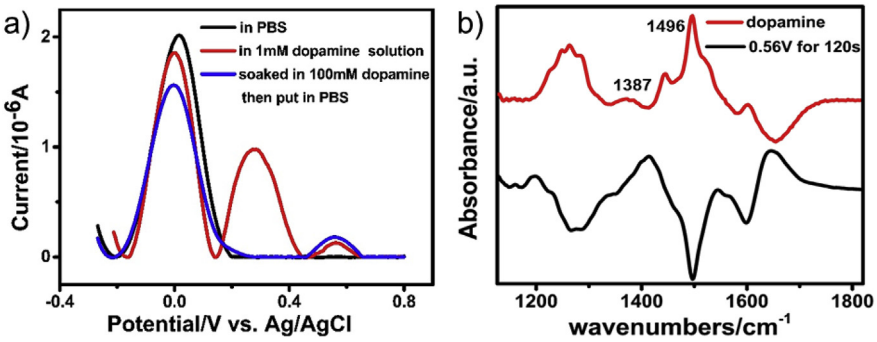

Fig. 3. a) DPVs of a poly(APBA-co-ABSA) modified electrode in 0.1 M PBS (pH 7.4) in the absence (black curve) and presence of 1 mM dopamine (red curve), and DPV of chemically bounded dopamine on poly(APBA-co-ABSA) from a 100 mM dopamine solution in PBS (blue curve). b) ATR-IR spectra of dopamine modified on the poly(APBA-co-ABSA) before and after electrochemical oxidation at 0.56 V (vs. Ag/AgCl) for 120 s.

released from the substrate, respectively (Figs. S6a and b). Therefore, 120 s is sufficient to release the captured cells. We also monitored the change of the substrate conductivity after cell release by EIS. Fig. S6c shows a remarkably increased R_{ct} after CTCs are captured on the substrate (black curve), which decreases as the captured cells are released from the substrate (green curve). It is noteworthy that the conductivity of substrate after cell release is higher than that of bare poly(APBA-co-ABSA) substrate (red curve). This is largely due to the remaining aptamer modified on the substrate, as indicated by the relatively high resistance of the aptamer-modified substrate (blue curve). It is noteworthy that our platform is promising to be reusable in the clinical application. After acid treatment and re-modification of the surface, the performance of substrate for cell capture and release seems unaffected (Fig. S6d). The viability of the released cells was evaluated by propidium iodide (PI)/acridine orange (AO) double staining analysis. Most of the released cells remain alive with a cell viability of 98% (Fig. S7), emphasizing that the present electrochemical approach combining with the poly(APBA-co-ABSA) surface is a promising noninvasive platform for cells capture/release.

Since the membrane protein of CTCs is important for the subsequent characterization, we investigated the tyrosine kinase 7 on the cell membrane of CCRF-CEM cells after release. FAM-labelled agc8c aptamer was used to monitor the tyrosine kinase 7. As shown in Fig. 5a, green fluorescence can be observed on the cell membrane of CCRF-CEM cells both before and after release. There is no obvious change in the intensity of the fluorescence of FAM after cell release, indicating that the mild potential perturbation will not reduce the amount of tyrosine kinase 7 expressed on the cell membrane of CCRF-CEM cells (Fig. 5b). These findings lead us to conclude that our method can efficiently release the captured cells without damaging the membrane protein of cells.

4. Conclusion

In summary, we have demonstrated a novel electrochemical strategy for controlled capture-and-release of cancer cells with high efficiency. The poly(APBA-co-ABSA) possesses a high degree of intermolecular self-doping, providing good conductivity to allow electrochemical release of cells at moderate potentials. Compared with the traditional approaches, the present electrochemical strategy shows advantages including ease of manipulation with rapid response and no harm to released cells. In addition, the cell capturing interface can be repeatedly utilized. We also illustrate the voltage-responsive mechanism of the DA-modified poly(APBA-co-ABSA) surfaces at the molecular level by ATR-IR. This novel system can be combined with conventional microfluidic devices to ultimately realize subsequent sorting and characterization of cancer cells by virtue of non-destructive and rapid release of attached cells. The proposed strategy is promising for biomedical research and clinical diagnostics in the future.

CRediT authorship contribution statement

Qian-Wen Zhang: Writing - original draft. **Jun Ouyang:** Methodology. **Yang Wang:** Project administration. **Ting-Ting Zhai:** Project administration. **Chen Wang:** Writing - review & editing. **Zeng-Qiang Wu:** Writing - review & editing. **Tian-Qi Zhang:** Project administration. **Kang Wang:** Writing - review & editing. **Xing-Hua Xia:** Supervision.

Acknowledgement

This work was supported by grants from the National Key R&D Program of China [2017YFA0700500]; the National Natural Science Foundation of China [21327902, 21635004, 21627806].

Appendix A. Supplementary data

Supplementary data to this article can be found online at https://doi.org/10.1016/j.bios.2019.111316.

Declaration of interests

None.

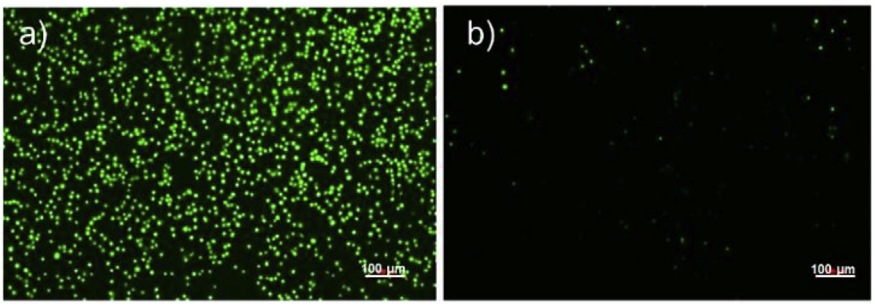

Fig. 4. Fluorescence images of cells captured on the poly(APBA-co-ABSA) surface before (a) and after (b) electrochemical oxidation at 0.6 V (vs. Ag/AgCl) for 120 s.

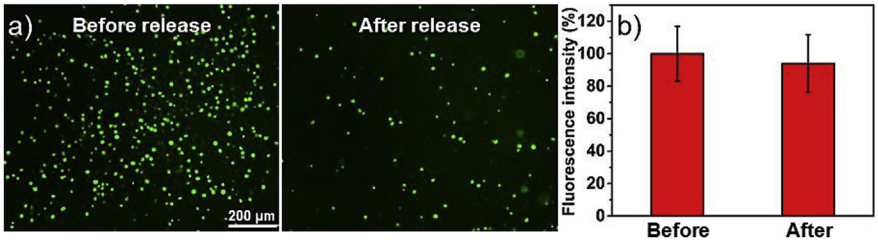

Fig. 5. a) The fluorescent images of CCRF-CEM cells incubated with AFM-labelled sgc8c aptamer before and after release. b) The quantitative analysis of CCRF-CEM cells incubated with AFM-labelled sgc8c aptamer before and after release.

References

Ao, Z., Parasido, E., Rawal, S., Williams, A., Schlegel, R., Liu, S., Albanese, C., Cote, R.J., Agarwal, A., Datar, R.H., 2015. Lab Chip 15 (22), 4277–4282.

Chambers, A.F., Groom, A.C., MacDonald, I.C., 2002. Nat. Rev. Canc. 2 (8), 563–572.

Chen, W., Cheng, Y., Wang, B., 2012. Angew. Chem., Int. Ed. Engl. 51 (22), 5293–5295.

Gao, T., Li, L., Wang, B., Zhi, J., Xiang, Y., Li, G., 2016. Anal. Chem. 88 (20), 9996–10001.

Green, B.J., Saberi Safaei, T., Mepham, A., Labib, M., Mohamadi, R.M., Kelley, S.O., 2016. Angew. Chem., Int. Ed. Engl. 55 (4), 1252–1265.

Hou, S., Zhao, H., Zhao, L., Shen, Q., Wei, K.S., Suh, D.Y., Nakao, A., Garcia, M.A., Song, M., Lee, T., Xiong, B., Luo, S.C., Tseng, H.R., Yu, H.H., 2013. Adv. Mater. 25 (11), 1547–1551.

Huang, Y.-J., Jiang, Y.-B., Fossey, J.S., James, T.D., Marken, F., 2010. J. Mater. Chem. 20 (38), 8305.

Ivanov, A.E., Panahi, H.A., Kuzimenkova, M.V., Nilsson, L., Bergenstahl, B., Waqif, H.S., Jahanshahi, M., Galaev, I.Y., Mattiasson, B., 2006. Chem. Eur J. 12 (27), 7204–7214.

James, T.D., Sandanayake, K., Shinkai, S., 1996. Angew. Chem. Int. Ed. 35 (17), 1910–1922.

Jiang, Y., Epstein, A.J., 1990. J. Am. Chem. Soc. 112 (7), 2800–2801.

Karyakin, A.A., Strakhova, A.K., Yatsimirsky, A.K., 1994. J. Electroanal. Chem. 371 (1–2), 259–265.

Kuralay, F., Sattayasamitsathit, S., Gao, W., Uygun, A., Katzenberg, A., Wang, J., 2012. J. Am. Chem. Soc. 134 (37), 15217–15220.

Labib, M., Green, B., Mohamadi, R.M., Mepham, A., Ahmed, S.U., Mahmoudian, L., Chang, I.H., Sargent, E.H., Kelley, S.O., 2016. J. Am. Chem. Soc. 138 (8), 2476–2479.

Lee, T.T., Garcia, J.R., Paez, J.I., Singh, A., Phelps, E.A., Weis, S., Shafiq, Z., Shekaran, A., Del Campo, A., Garcia, A.J., 2015. Nat. Mater. 14 (3), 352–360.

Li, Y., Xiao, W., Xiao, K., Berti, L., Luo, J., Tseng, H.P., Fung, G., Lam, K.S., 2012. Angew. Chem., Int. Ed. Engl. 51 (12), 2864–2869.

Li, W., Wang, J., Ren, J., Qu, X., 2013. Angew. Chem., Int. Ed. Engl. 52 (26), 6726–6730.

Li, W., Reategui, E., Park, M.H., Castleberry, S., Deng, J.Z., Hsu, B., Mayner, S., Jensen, A.E., Sequist, L.V., Maheswaran, S., Haber, D.A., Toner, M., Stott, S.L., Hammond, P.T., 2015. Biomaterials 65, 93–102.

Liu, D., Xie, Y., Shao, H., Jiang, X., 2009. Angew. Chem., Int. Ed. Engl. 48 (24), 4406–4408.

Liu, H., Li, Y., Sun, K., Fan, J., Zhang, P., Meng, J., Wang, S., Jiang, L., 2013. J. Am. Chem. Soc. 135 (20), 7603–7609.

Ng, C.C., Magenau, A., Ngalim, S.H., Ciampi, S., Chockalingham, M., Harper, J.B., Gaus, K., Gooding, J.J., 2012. Angew. Chem., Int. Ed. Engl. 51 (31), 7706–7710.

Nie, H., Chen, Y., Lu, C., Liu, Z., 2013. Anal. Chem. 85 (17), 8277–8283.

Nishiyabu, R., Kubo, Y., James, T.D., Fossey, J.S., 2011. Chem. Commun. 47 (4), 1124–1150.

Ouyang, J., Chen, M., Bao, W.-J., Zhang, Q.-W., Wang, K., Xia, X.-H., 2015. Adv. Funct. Mater. 25 (38), 6122–6130.

Parkinson, D.R., Dracopoli, N., Petty, B.G., Compton, C., Cristofanilli, M., Deisseroth, A., Hayes, D.F., Kapke, G., Kumar, P., Lee, J.S.H., Liu, M.C., McCormack, R., Mikulski, S., Nagahara, L., Pantel, K., Pearson-White, S., Punnoose, E.A., Roadcap, L.T., Schade, A.E., Scher, H.I., Sigman, C.C., Kelloff, G.J., 2012. J. Transl. Med. 10, 20.

Persson, K.M., Karlsson, R., Svennersten, K., Loffler, S., Jager, E.W., Richter-Dahlfors, A., Konradsson, P., Berggren, M., 2011. Adv. Mater. 23 (38), 4403–4408.

Plaks, V., Koopman, C.D., Werb, Z., 2013. Science 341 (6151), 1186–1188.

Poudineh, M., Labib, M., Ahmed, S., Nguyen, L.N.M., Kermanshah, L., Mohamadi, R.M., Sargent, E.H., Kelley, S.O., 2017. Angew. Chem., Int. Ed. Engl. 56 (1), 163–168.

Reategui, E., Aceto, N., Lim, E.J., Sullivan, J.P., Jensen, A.E., Zeinali, M., Martel, J.M., Aranyosi, A.J., Li, W., Castleberry, S., Bardia, A., Sequist, L.V., Haber, D.A., Maheswaran, S., Hammond, P.T., Toner, M., Stott, S.L., 2015. Adv. Mater. 27 (9), 1593–1599.

Robertus, J., Browne, W.R., Feringa, B.L., 2010. Chem. Soc. Rev. 39 (1), 354–378.

Schiro, P.G., Zhao, M., Kuo, J.S., Koehler, K.M., Sabath, D.E., Chiu, D.T., 2012. Angew. Chem., Int. Ed. Engl. 51 (19), 4618–4622.

Shah, A.M., Yu, M., Nakamura, Z., Ciciliano, J., Ulman, M., Kotz, K., Stott, S.L., Maheswaran, S., Haber, D.A., Toner, M., 2012. Anal. Chem. 84 (8), 3682–3688.

Wan, Y., Zhou, Y.G., Poudineh, M., Safaei, T.S., Mohamadi, R.M., Sargent, E.H., Kelley, S.O., 2014. Angew. Chem., Int. Ed. Engl. 53 (48), 13145–13149.

Wang, M., Xiao, F.-N., Wang, K., Wang, F.-B., Xia, X.-H., 2013. J. Electroanal. Chem. 688, 304–307.

Wang, S., Ye, J., Bie, Z., Liu, Z., 2014. Chem. Sci. 5 (3), 1135.

Wischerhoff, E., Uhlig, K., Lankenau, A., Borner, H.G., Laschewsky, A., Duschl, C., Lutz, J.F., 2008. Angew. Chem., Int. Ed. Engl. 47 (30), 5666–5668.

Wu, W., Zhu, H., Fan, L., Liu, D., Renneberg, R., Yang, S., 2007. Chem. Commun. 23, 2345.

Yoon, H.J., Kozminsky, M., Nagrath, S., 2014. ACS Nano 8 (3), 1995–2017.

Zhang, L., Kerszulis, J.A., Clark, R.J., Ye, T., Zhu, L., 2009. Chem. Commun. (16), 2151–2153.

Zhang, P., Chen, L., Xu, T., Liu, H., Liu, X., Meng, J., Yang, G., Jiang, L., Wang, S., 2013. Adv. Mater. 25 (26), 3566–3570.

Zhong, X., Bai, H.-J., Xu, J.-J., Chen, H.-Y., Zhu, Y.-H., 2010. Adv. Funct. Mater. 20 (6), 992–999.